Development of fast image analysis technique for All-Sky images

A. K. Sharma[1], D. P. Nade[1,*], S. S. Nikte[1], R. N. Ghodpage[2], P. T. Patil[2], M. V. Rokade[1], R. S. Vhatkar[1] and S. Gurubaran[3]

[1]Earth and Space Science Laboratory, Department of Physics, Shivaji University, Kolhapur 416 004, India
[2]Medium Frequency Radar, Indian Institute of Geomagnetism, Shivaji University Campus, Kolhapur 416 004, India
[3]Indian Institute of Geomagnetism, New Panvel, Navi Mumbai 410 218, India

This article describes the possibility of using the fast image analysis technique for qualitative and quantitative analysis of equatorial plasma bubble obtained using All-Sky imager (ASI) data. Automated image processing (generally) is useful for identification of equatorial plasma bubbles (EPBs) and its parameters. We have developed a fast (and efficient) analysis technique essential to study the data of images. The present work reports the results of a statistical study of the zonal plasma bubble velocities using nightglow OI 630.0 nm emission data, acquired by ASI (FOV 140º) at the low-latitude station Kolhapur (16.42°N, 74.2°E and 10.6°N dip lat.). Based on the observations of 15 nights made in January 2012, we have determined the velocity of EPB using our new method. The daily mean values of the EPB velocity match well with those of the earlier studies made at Kolhapur. We have found that, generally, the mean zonal drift velocities of the plasma bubbles tend to decrease with local time (after midnight). The most significant finding from this work is that the calculated velocities of plasma bubble using fast and scanning methods are nearly equal.

Keywords: All-Sky imager, equatorial plasma bubble, nightglow emissions, zonal drift velocity.

THE part of Earth's atmosphere (above about 60 km) where the free electrons and ions exist in numbers sufficient to influence the travel of radio wave is called the ionosphere. Large-scale ionospheric irregularities are observed in the F-region due to depleted density of electrons, known as plasma bubble. This electron density can contribute to airglow[1] at a height ~300 km. Plasma bubbles have played a major role in the equatorial spread-F (ESF) phenomenon[2]. Here the electrons move faster than acoustic velocity in the medium. The plasma moves from the region of the magnetic equator to either side in the range ±10° to ±20° north and south of the magnetic equator and covers north–south distances across the magnetic equator of several thousand kilometres, with east–west dimensions of up to a few hundred kilometres[3].

*For correspondence. (e-mail: dada.nade@gmail.com)

As India hosts not only the tropical region but also the geomagnetic ionization anomaly, the specificity of the region should be recognized and features such as the large horizontal ionization gradients and day-to-day variability in the prediction of ionospheric parameters must be considered[4]. At Kolhapur, a CCD-based All-Sky imaging system with three different filters for night airglow emission lines (OI 630.0 nm, 557.7 nm and OH), has been used to study the upper atmosphere of the Earth that provides information over a much larger field of view (FOV) of 180°. This system is capable of viewing large-scale plasma bubbles over a large geographical area (~1,200,000 sq. km at an altitude of 250 km) from Kolhapur (16.8°N, 74.2°E and 10.6°N dip lat.). The advantages of the All-Sky imager (ASI) over other instruments (which are used to study the upper atmosphere) are that it can resolve individual small-scale gravity wave events and large-scale plasma bubble events[5]. Figure 1 shows the area covered by ASI with limited FOV of 140° from Kolhapur, assuming an airglow emission at height of 250 km. The observed column of OI 630.0 nm emission intensity is proportional to the integral of

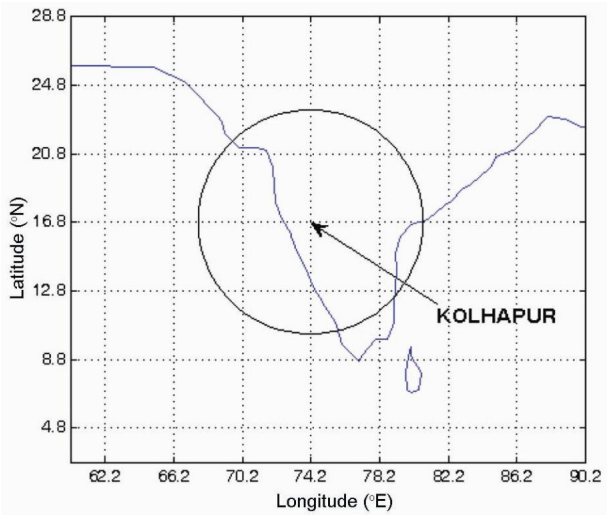

Figure 1. Area covered by All-Sky imager having field of view 140° from Kolhapur at an altitude of 250 km where 630.0 nm emissions are generated.

the product of O_2^+, e (electron density) and charge transfer concentrations[3]. The F-region nightglow OI 630.0 nm emission line arising from dissociative recombination: $O_2^+ + e \rightarrow O + O^*$ (refs 6 and 7) and radiative recombination: $O^+ + e \rightarrow O^* + h\nu$ which leads to $O^* \rightarrow O + h\nu_{(630\,nm)}$ processes respectively can be used to observe plasma bubbles and to study their development and dynamics.

Plasma drifts in the equatorial region have been widely studied using satellite and ground-based techniques. In ground-based techniques, mostly photometer[7–10] and advanced ASI[3,8,11–18] are used to study the ionospheric irregularities by OI 630.0 nm emission line, which is generated at an altitude 250 km. The ground-based measurements of various F-region and mesospheric nightglow emissions [OI 630 nm, 557.7 nm, 777.4 nm, Na (589.3 nm) and hydroxyl (OH) airglow] provide important information of the ionosphere–thermosphere during the different phases of a geomagnetic storm. Limited studies have been made on ionospheric plasma bubble using ASI in the Indian region.

The dimensions[11] and circulation path[19] of the plasma depletions or bubbles were first studied in the Indian sector by OI 630.0 nm airglow emission using ASI. The zonal velocity of the plasma bubble depends on the solar activities, local time[10,19], geomagnetic storm[15] and latitude–longitude variations[17]. Converging zonal winds are commonly observed during night. It can affect the ESF plume in such a way that upward $E \times B$ drifts cease. The neutral winds are responsible for the ESF phenomenon[1].

In this article, we introduce the high-resolution ASI set-up at Kolhapur (India) and discuss the image processing and analysis method. We have developed a formula for conversion of pixel coordinate to geographic coordinate of All-Sky images, based on simple airglow geometry viewed by ASI. Using this method, we have analysed data of the image of January 2012.

Instrument

All-Sky Imager

The imaging system was installed in 2009 under the scientific collaboration programme between Shivaji University, Kolhapur and Indian Institute of Geomagnetism, Navi Mumbai at Shivaji University Campus, Kolhapur (16.42°N, 74.2°E and 10.6°N dip lat.). The ASI is being used to observe the atmospheric airglow features to study the ionospheric irregularities. A schematic of optical ray paths of ASI is shown in Figure 2. The system is composed of mainly three parts:

(i) *Optical part:* This consists of fish eye lens (f/4 Mamiya RB67) with focal length 24 mm, a telecentric optical lens combination and a filter wheel. The 180° FOV fish eye lens collects lights from the Earth's upper atmosphere for different altitudes. The collected light beam is collimated by a telecentric optical lens combination. Then it passes through a narrow-band filter with nearly perpendicular incident angles[14]. The six filters are built in the filter wheel to allow the transmission of OI 630.0 nm, OI 557.7 nm, 840.0 nm, 846.0 nm and OH Meinel bands at 720.0–910.0 nm and the transmission of background light at 857.0 nm. Their sampling rates are 120, 120, 06, 06, 90 and 10 sec respectively.

(ii) *Detector:* CCD camera and detector is thermo-electrically cooled at –80°C to reduce thermal noise. The collimated beam falls on the CCD detector through the filter wheel to make an image. The CCD (13.3 × 13.3 mm to 27.6 × 27.6 mm) detector is back-illuminated with an array of 1024 × 1024 pixels (quantum efficiencies better than 95%) and 16 bits resolution (for 16 bit image 65,535 corresponds to white and 0 bit corresponds to black colour). The CCD response is almost flat and differential gain of pixel is merely statistical in nature[5].

(iii) *Operating system:* The filter wheel, camera shutter and cooling system are controlled by a notebook PC (HP) with the Windows XP operating system.

Image processing

An image taken by ASI is not appropriate for the normal 2D spectral analyses. Image processing is necessary to identify airglow events in the image. Several methods of image processing are reported in the literature. Image processing and its spectral analysis were first described by Garcia *et al.*[20], to study gravity wave parameters

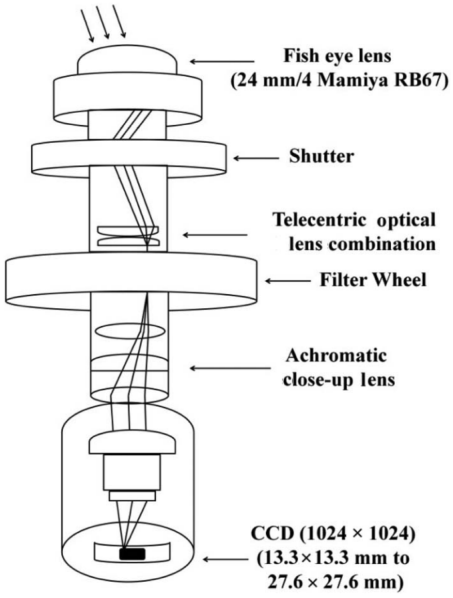

Figure 2. Schematic of the All-Sky imager with optical ray paths.

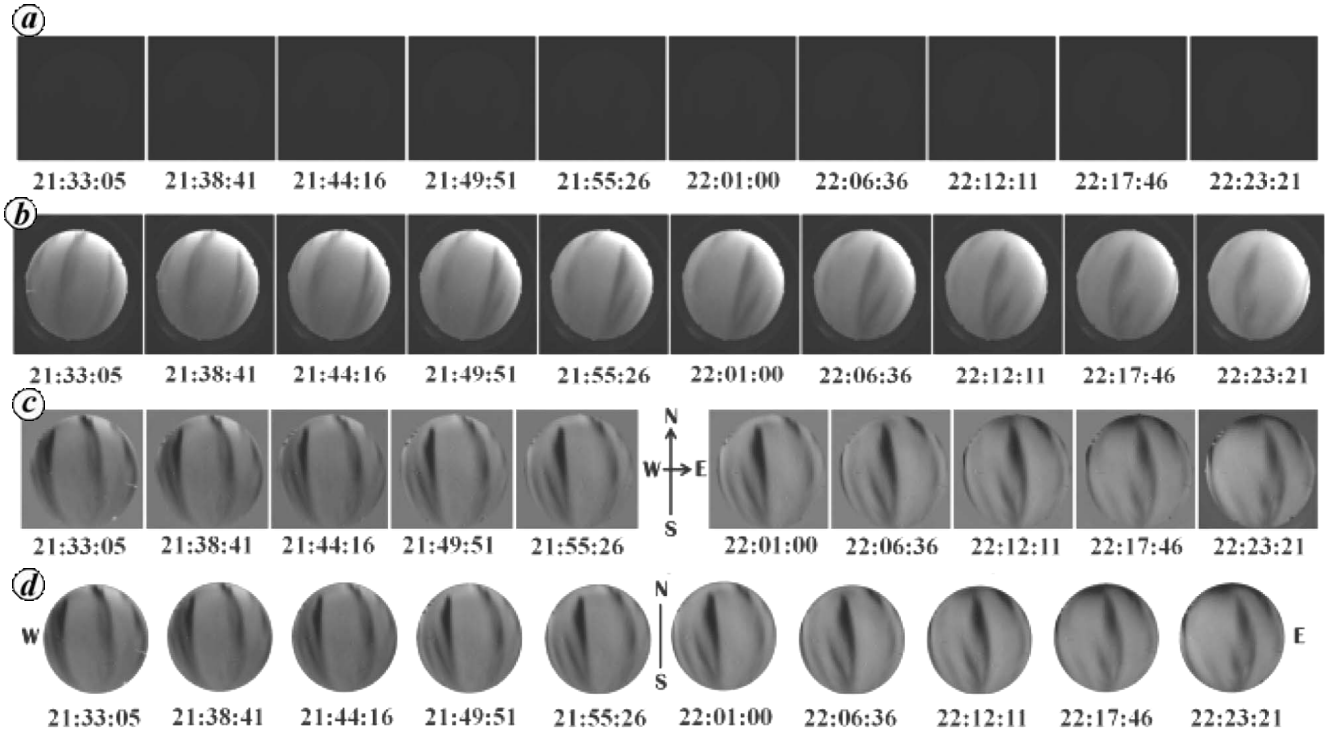

Figure 3. Image processing steps. ***a***, OI 630.0 nm images (in PNG format) were taken by All-Sky imager on 20/01/2012 from 21:33:05 to 22:33:21 LT. ***b***, Auto level images. ***c***, After this processing, images were tilted by 8.2° and flip horizontally for correction of image direction. ***d***, Cropped image.

(wavelength, velocity and period) from All-Sky images. Based on this image processing, Pimenta *et al.*[13] introduced image scanning method to study the internal space–time dynamics of plasma bubble. The fundamental of image processing has been described briefly by Seker *et al.*[16]. As reported in the literature, image processing includes mostly dark count correction, star removal and Van Rhijn effect. The image appears curved and compressed at low elevation angles. This occurs because the lens projects an image onto the CCD such that each pixel subtends an equal angle of the sky[13]. It is necessary to develop an efficient image processing method for clear identification of wave-like structure (in OH and OI 557.7 nm emission line) and plasma depletions (in OI 630.0 nm emission line). The flat fielding of image is the main principle of image processing[20], which is useful for image analysis.

In the present study we have introduced a simple image processing and averaging method. Figure 3 illustrates the steps involved in image processing for the nightglow OI 630.0 nm images taken by ASI during clear moonless night on 20–21 January 2012 during 21:33:05 to 22:23:21 LT (local time = universal time + 5:30 h). This process uses CCD Stack software. The images were taken PNG (portable network graphics) format (Figure 3 *a*). We have first converted these PNG files into TIFF (tagged image file format) using Adobe Photoshop CS2 since CCD Stack cannot work with PNG files. After conversion, TIFF images were auto-levelled by Adobe Photoshop CS2 (Figure 3 *b*). We have checked and found that the resolution and pixel value (1024 × 1024) of the image do not change due to this process. We have taken the mean/average of an hour image-data, and then subtract this (averaged image) mean image from each image of an hour data (Figure 3 *c*). Due to this process we can easily identify the edges of the plasma bubble in OI 630.0 nm images. After this processing, images were tilted by 8.2° and flip horizontally for correct direction (Figure 3 *c*). Figure 3 *d* shows the cropped images for only airglow data recorded by ASI.

Image analysis

Figure 4 shows the geometry of nightglow emission layer viewed by ASI from the surface of the Earth. The airglow emissions originated at a mean height h above the surface of the Earth. An observer, at point A, is observing airglow structure at a point B, as shown in Figure 4. According to vector addition theorem, we can write the following equation using geometry of airglow emission layer

$$r = (R_h^2 - R^2 - 2rR\cos\theta)^{1/2}, \quad (1)$$

where $R_h = R + h$, R is the mean radius of the Earth and θ is the zenith angle which varies up to 90° since FOV of

Table 1. Parameters of the airglow geometry

Field of view (°)	θ°	ϕ°	α°	ψ°	Pixel size	r (km)	Pixel value (km)	Acre (km)	a (km)	A (km^2)
20	10	80	89.806	0.389	113.770	253.700	0.790	44.945	44.945	6,346.240
40	20	70	89.607	0.7855	227.550	265.380	0.798	90.757	90.757	25,876.489
60	30	60	89.379	1.2415	341.330	286.880	0.840	143.444	143.441	64,639.276
80	40	50	89.104	1.7923	455.110	322.120	0.910	207.084	207.075	134,712.058
100	50	40	88.713	2.5737	568.890	379.020	1.045	297.367	297.342	277,755.883
120	60	30	88.221	3.5586	682.670	474.470	1.204	411.163	411.097	530,932.269
140	70	20	87.358	5.2834	796.450	648.710	1.532	610.448	610.232	1,169,875.608
160	80	10	85.680	8.6271	910.230	1008.340	2.188	996.782	995.841	3,115,512.722
180	90	0	82.105	15.79	1024.000	1802.080	3.552	1824.389	1818.621	10,390,451.500

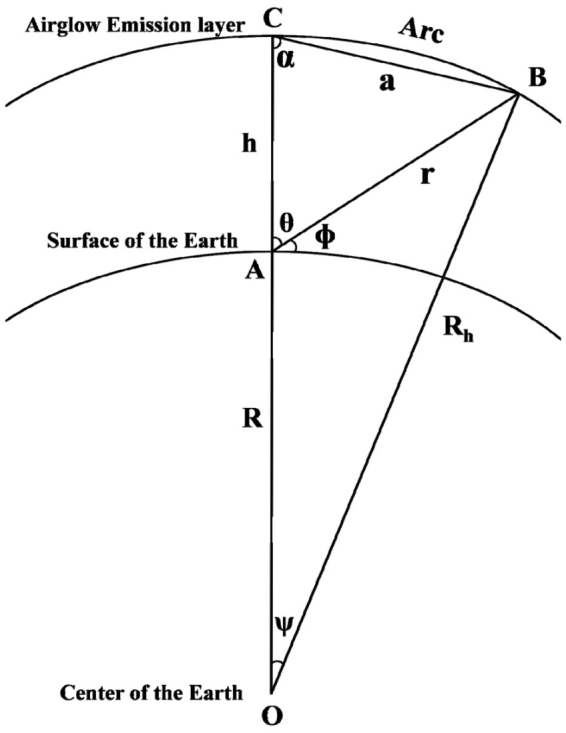

Figure 4. Geometry of airglow emission layer viewing by All-Sky imager.

ASI is 180°. Thus, we consider the values of zenith angle to vary from 10° to 90°. For these values of zenith angle, we calculate the corresponding distance between airglow structure (B) and observer (A) using eq. (1). Table 1 gives the value of r. Here r is the distance between the observatory and the mark of airglow emission in the sky. Once the values of r are known, we can determine the Earth-centred angle ψ using the following equation

$$\psi = \cos^{-1}\left(\frac{R_h^2 + R^2 - r^2}{2R_h R}\right). \quad (2)$$

Using eq. (2), we can determine a, the distance of airglow event from zenith at an altitude h by the geometry illustrated in Figure 4.

$$a = [2R_h^2(1-\cos\psi)]^{1/2}. \quad (3)$$

However, the nature of airglow emission layer is spherical around the Earth. Thus, by two-dimensional viewing, airglow emissions make a circle having radius $(R + h)$ with centre at O (centre of the Earth). Using the formula for arc, we can accurately determine the distance between zenith and signature of airglow emission. The equation for arc is as follows

$$\text{Arc} = \text{Radius} \times \text{Angle} = R_h \times \psi. \quad (4)$$

The size of the projected pixels varies considerably with elevation and the shapes are dependent on the viewing azimuth[20]. Thus, the pixel value of the image depends on FOV of the imager and altitude of airglow emission layer. So before quantitative analysis, All-Sky images were converted into geographic coordinates by assuming an altitude of the airglow emission layer[21]. In the present work, we considered the altitude of airglow emission layer to be 250 km, where the OI 630.0 nm emissions are assumed to have originated. Once we know the value of ψ, we can determine the length of airglow emission structure from the zenith. From Kolhapur, ASI covers a zenith angle range of about 70° (140° FOV) (and not 90° (180° FOV)) because of local sky-viewing conditions. Thus, we draw a circle on the image having radius a with centre at zenith (512, 512) and convert the value of a into kilometre using eq. (3). Then comparing diameter of the image with corresponding original pixel size of the CCD image, we can convert the value of one pixel into kilometre. The calculated parameters of airglow geometry are summarized in Table 1. At Kolhapur, All-Sky image covered approximately ±6° latitude and longitude from the zenith. This corresponds to a horizontal distance of about ~1220 km diameter at an altitude of 250 km. In the present work we have used the OI 630.0 nm images to study the plasma bubble. So for 140° FOV, the value of one pixel is 1.533 km. Elevation angle is the linear function of OI 630.0 nm nightglow emission layer about 50° at an altitude 250 km, and OH and OI 557.7 nm emission layer about 40° at an altitude 96 km (ref. 20).

After converting pixel values into corresponding latitude–longitude values of airglow emission height[5], the velocity and other parameters of plasma depletion were retrieved from successive images[22]. A CCD-based ASI recorded OI 630.0 nm images having 1024 × 1024 pixels, centre of image at 512, 512 pixels. Considering this centre of image, we drew the circle on the cropped image (Figure 5 *a*); as a result the image is divided into four quadrants. The zenith, centre of image (512, 512 pixels), indicates the location of the observatory, Kolhapur (16.42°N, 74.2°E and 10.6°N dip lat.), as shown in Figure 1. The spatial location is important to identify the direction of plasma depletion; the upward portion of the image is considered as north direction and right side as east direction. To calculate the velocity of plasma bubble, we traced its position in successive images. Figure 5 shows the edges (eastern wall, western wall and centre) of the plasma bubble. Herein we have taken average motion of the eastern wall, centre and western wall of the plasma bubble; these values are again averaged. The traced position of the western wall, centre and eastern wall of the plasma bubble are shown in Figure 5 *b*, *c* and *d* respectively. All the analyses are mostly automated and hence we call this the 'fast method'.

Observations and data

Regular observations of the OI 630.0 nm nightglow emissions, with 120 sec sampling rate (image repetition rate 345 sec), have been carried out during clear moonless nights from Kolhapur since 2009. In the present work, we have taken OI 630.0 nm image data for January 2012. Typically, observations began approximately 1 h after sunset and ended 1 h before sunrise. Depending on season, start time was between ~19:30 and ~20:00 LT, and end time was between 4:30 and 5:30 LT. During January 2012, relatively good sequences of observations were taken on 15 successive nights. Out of these, ten nights showed optical signatures of large-scale, nearly north–south field-aligned, plasma depletions/bubbles in the equatorial F-region. During this period, about 1672 images of OI 630.0 nm were recorded by ASI from Kolhapur. About 707 images (42.28%) showed the presence of quasi N–S-aligned depleted intensity regions and out of these, 220 images (31.11% images) showed very good plasma events during time slot of 21:30–00:00 LT. Details of the nightglow observations of plasma bubble during January 2012 are summarized in Table 2. Large-scale ionospheric plasma depletions were observed at different times during a night and under both magnetically disturbed and quiet conditions. The north–south aligned plasma bubbles propagated towards the east throughout the nights. Four nights 17–18, 18–19, 20–21 and 21–22 January 2012 were selected to study the nocturnal variation in zonal motion of plasma bubble as a case study.

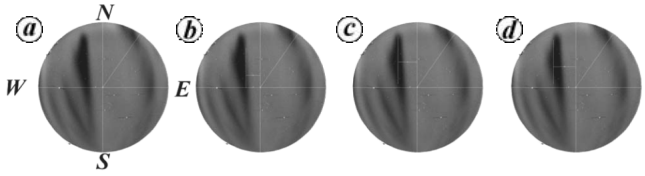

Figure 5. Image analysis. (***a***) Four quadrants of the image with centre (512, 512) zenith, (***b***) eastern wall, (***c***) centre and (***d***) western wall of the plasma bubble.

The purpose of the present study is to introduce and verify the new image analysis method and to carry out a geometric study of the zonal plasma bubble velocities using the same. Herein we have compared our method with that of described by Pimenta *et al.*[13]. The fast image analysis method seems more accurate than the scanning method to determine the velocity of the plasma bubble.

Results and discussion

The present study is based on observations, made during 15 nights, of the nightglow OI 630.0 nm emission by ASI from Kolhapur. Out of these, observations for four nights are selected for correlation analysis because nearly 6 h event data were available only for these nights, i.e. 17–18, 18–19, 20–21 and 21–22 January 2012. Extensions of bottom-side ionospheric plasma bubbles into topside ionosphere across the entire equatorial region[23] are observed in two-dimensional images of nightglow OI 630.0 nm emission. From the spatial displacements of the plasma bubbles, in successive images, we can infer the zonal drift velocities.

Peminta *et al.*[13] introduced the methodology to determine the zonal velocity of plasma bubble using nightglow OI 630.0 nm All-Sky images. Based on this method, we first scanned the optical images through the zenith (16.8°N) from east to west to obtain a cross-section of the depletion patterns for each plasma bubble. Then, these cross-sectional scans were subjected to an analysis; a succession of spatial space and time shifts leads to a zonal velocity versus local time relation for the plasma bubble. For this method we have taken only those images having plasma bubbles at or near the zenith (in 100° FOV). Figure 6 *a* and *b* illustrates the east-west scan of depletion region obtained in nightglow OI 630.0 nm images at 21:10:45, 21:16:20, 21:21:55, 22:01:00, 22:06:36 and 22:12:11 LT on 20–21 January 2012. The east–west scanned data are smoothed by 50 points average to recognize the boundaries of plasma bubbles (Figure 6 *c* and *d*). In nightglow OI 630.0 nm intensity (arb. units) plot, the black arrows (pointing upwards) indicate the centre of the plasma bubble. From the special displacements of these depletion regions, we can determine its velocity.

Table 2. Observation of nightglow OI 630.0 nm images by All-Sky imager during January 2012 from Kolhapur

Date	Total images	Event images	Period of good events	Number of good event images
17–18/01/2012	113	54	21:12:31–24:28:18 LT	35
18–19/01/2012	125	104	21:33:47–24:48:04 LT	39
19–20/01/2012	113	110	20:30:09–22:25:05 LT	21
20–21/01/2012	111	111	20:31:39–24:26:11 LT	43
21–22/01/2012	109	90	22:32:53–24:27:49 LT	21
22–23/01/2012	108	26	–	
23–24/01/2012	164	127	20:56:10–22:50:40 LT	30
24–25/01/2012	113	33	20:48:17–21:53:50 LT	16
25–26/01/2012	114		Event not observed	
26–27/01/2012	124	35	21:32:22–23:25:53 LT	15
27–28/01/2012	114	17		
28–29/01/2012	92		Event not observed	
29–30/01/2012	98		Cloudy conditions	
30–31/01/2012	82		Cloudy conditions	
31/01–01/02/2012	92		Event not observed	

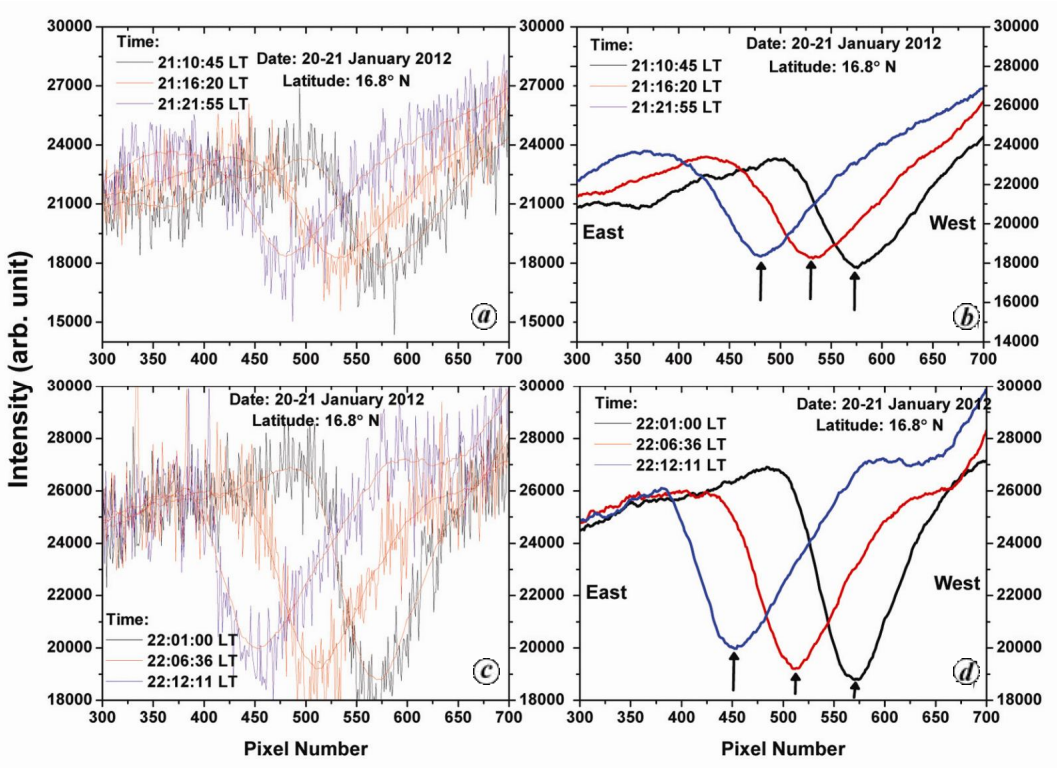

Figure 6. East–west scan of depletion obtained in successive images of nightglow OI 630.0 nm at different times on 20–21 January 2012. The east–west scanned data smoothed by 50 points averaged and black arrow (pointing upwards) show the depletion in nightglow OI 630.0 nm intensity (arb. units).

We have determined motion of western wall, centre and eastern wall of plasma bubble using scanning and fast method for 17–18 and 20–21 January 2012 nights. In Figure 7, the motion of these are indicated by black, red and blue lines respectively, on 17–18 and 20–21 January 2012, by scanning method (Figure 7 *a* and *b*) and by fast method (Figure 7 *c* and *d*). It is clear from Figure 7 that determined velocity of western wall, centre and eastern wall of plasma bubble using scanning method shows large variations than that using fast method. So, the fast method is more accurate than the scanning method to determine the velocity of plasma bubble by nightglow OI 630.0 nm All-Sky images.

For more accurate determination of the plasma bubble velocity, we have taken the average of its western wall, centre and eastern wall velocities. The average velocities of plasma bubble determined using both methods for January 2012 are summarized in Table 3, which shows

Table 3. Averaged velocity of plasma bubble calculated by fast and scanning methods for January 2012

Date	Fast method (m/s)	Scanning method (m/s)	Date	Fast method (m/s)	Scanning method (m/s)
17–18/01/2012	123	126	22–23/01/2012	206	220
18–19/01/2012	113	121	23–24/01/2012	102	114
19–20/01/2012	115	120	24–25/01/2012	178	188
20–21/01/2012	169	187	26–27/01/2012	208	215
21–22/01/2012	178	190	27–28/01/2012	161	167

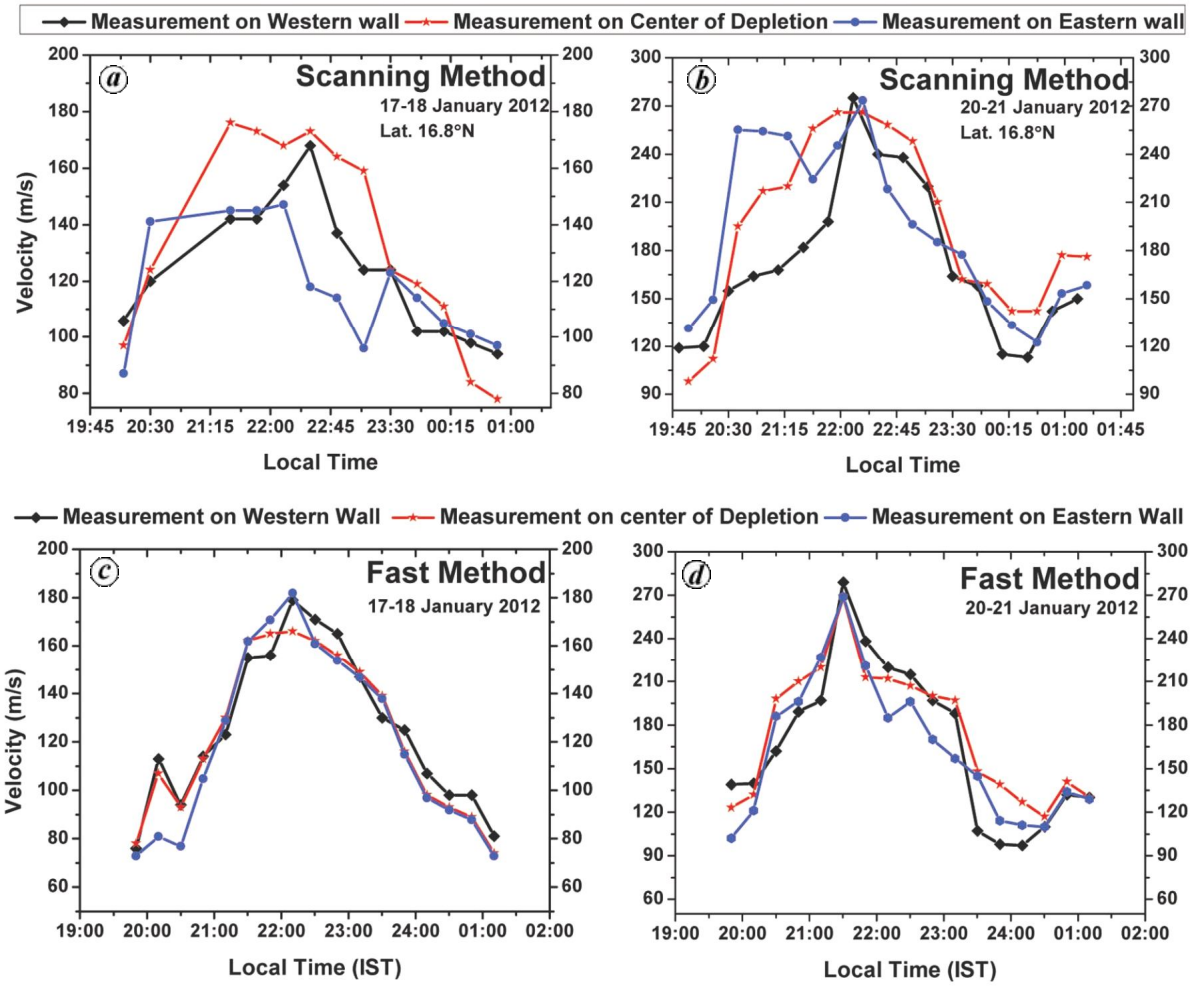

Figure 7. Motion of western wall, centre and eastern wall of plasma bubble for 17–18 and 20–21 January 2012.

that calculated velocities by both the methods are nearly equal. Figure 8 illustrates the averaged and mean standard deviations of plasma bubble velocity calculated using scanning and fast methods indicated by black and blue lines respectively, for 17–18, 18–19, 20–21 and 21–22 January 2012 nights. From Figure 8, it is confirmed that calculated velocities of plasma bubble by both methods are nearly equal.

The average zonal velocities of plasma bubbles are about 151.22 and 171.97 m/s around 20:30 LT and then tend to decrease with local time. The eastward zonal velocities decrease after midnight[24]. After sunset, the growth of ionospheric plasma instabilities or the equatorial upward plasma drift is driven by the F-layer dynamo by zonal (eastward) electric field[25]. The intensity of this electric field is very intense after sunset and decreases with time because of the reduced neutral wind velocity[10]. This result can be understood by the fact that the electric field polarization of the F-region drives the nocturnal zonal drift of the plasma in that region.

We have observed zonal velocities of plasma bubble eastward throughout the night, in the same direction as

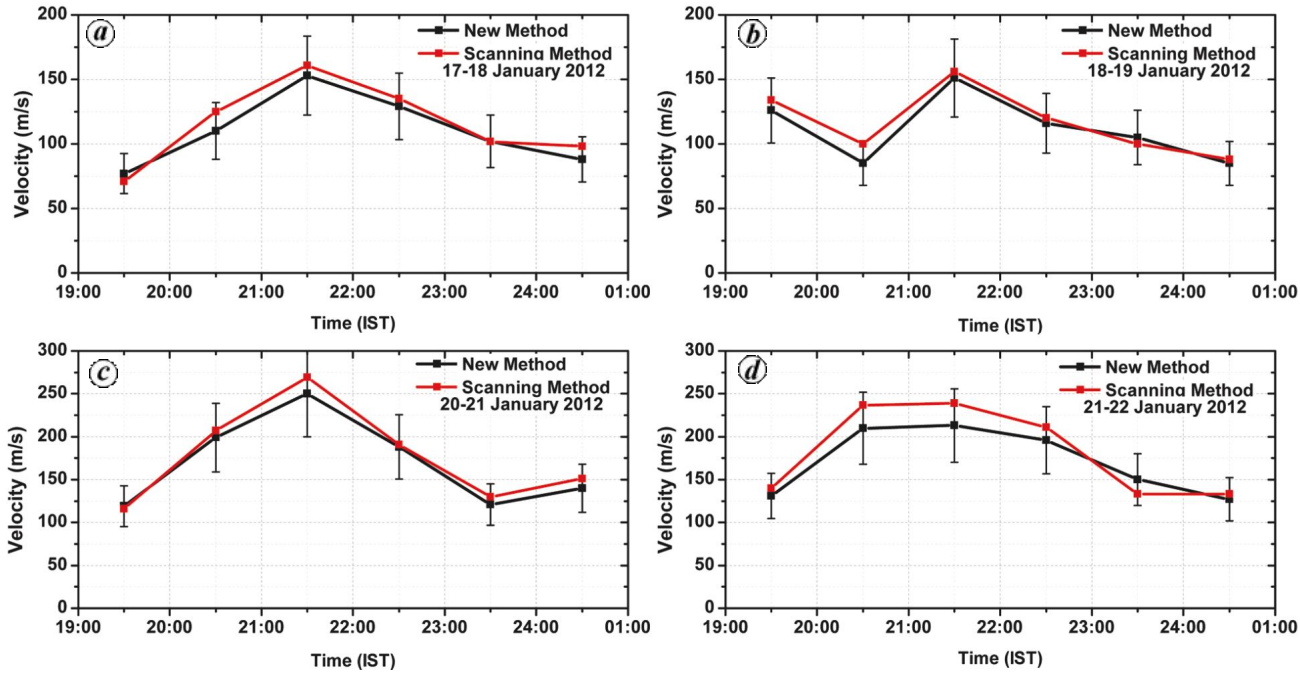

Figure 8. Averaged and mean standard deviation of plasma bubble velocity as a function of local time.

the F layer neutral winds, to increase before midnight (21:00–22:00 LT) and then decrease with local time. This result is in agreement with that of the Mukherjee *et al.*[11] and Daniela *et al.*[26]. In the night-time equatorial F-region, the eastward neutral wind develops a vertically downward polarization electric field, which drives the plasma eastward. The zonal plasma velocities depend essentially on the intensity of the zonal wind velocity[27,28]. But Terra *et al.*[10] and Martinis *et al.*[17] have assumed that both the EPBs and the background plasma drift motions are the same with zonal velocity and its structure becomes strongly coupled to the zonal drifts. The plasma zonal velocities normally have eastward movement relative to the ground and during some magnetic storms, this movement changes to the west[29]. However, there are some rare cases of plasma bubbles moving to the west during magnetically quiet nights, as reported by Sobral *et al.*[30]. Before about 21:00 LT, the ionospheric irregularities are still influenced by the growing phase, when they are strongly dominated by electrodynamic forces that make their velocities different from the large-scale ionospheric velocity[29].

Conclusion

The All-Sky Imager at Kolhapur is a useful tool in ionospheric research. The results of the present study are summarized below.

(a) We have shown here how to use ASI data for qualitative and quantitative analysis of equatorial plasma bubble by nightglow OI 630.0 nm images.

(b) Automatic image processing is useful for identification of EPB and its parameters such as length, width of EPBs.

(c) We have developed an efficient analysis technique which is important for studies of All-Sky image data. The hourly mean velocities of plasma bubble were nearly equal for four nights using fast and scanning methods.

(d) Nightglow OI 630.0 nm images were obtained by ASI (FOV 140°) at the low-latitude station Kolhapur, based on 15 nights of experiments during January 2012. We determined average zonal velocities of plasma bubbles to be about 151.22 and 171.97 m/s around 20:30 LT, which then tend to decrease with local time.

(e) The velocities were found to peak (maximize) before midnight, i.e. between 21:30 and 20:30 LT during January 2012. It was also observed that these velocities tend to decrease faster with local time after midnight.

1. Krall, J., Huba, J. D. and Martinis, C. R., Three-dimensional modeling of equatorial spread F airglow enhancements. *Geophys. Res. Lett.*, 2009, **36**, L10103; doi: 10.1029/2009GL038441.
2. Tsunoda, R. T., Livingston, R. C., McClure, J. P. and Hanson, W. B., Equatorial plasma bubbles: vertically elongated wedges from the bottomside F layer. *J. Geophys. Res. A*, 1982, **87**(A11); doi: 10.1029/0JGREA000087000A11009171000001.
3. Sahai, Y., Fagundes, P. R., Abalde, J. R., Pimenta, A. A., Bittencourt, J. A., Otsuka, Y. and Rios, V. H., Generation of large-scale equatorial F-region plasma depletions during low range spread-F season. *Ann. Geophys.*, 2004, **22**, 15–23.
4. Pillai, K. G. M., Dabas, R. S., Veenadhari, B. and Lakshmi, D. R., The scientific basis for solar–terrestrial prediction at National

Physical Laboratory, New Delhi. *J. Indian Geophys. Union*, 2003, **3**, 159–169.
5. Narayanan, V. L., Gurubaran, S. and Emperumal, K., Imaging observations of upper mesospheric nightglow emissions from Tirunelveli (8.7°N). *Indian J. Radio Space Phys.*, 2009, **38**, 150–158.
6. Mukherjee, G. K. and Shetti, D. J., Plasma drift motion in F-region of ionosphere using photometric nightglow measurements. *Indian J. Radio Space Phys.*, 2008, **37**, 249–257.
7. Mukherjee, G. K., Carlo, L. and Mahajan, S. H., 630 nm nightglow observations from 17°N latitude. *Earth Planets Space*, 2000, **52**, 105–110.
8. Mukherjee, G. K., The signature of short-period gravity waves imaged in the OI 557.7 nm and near infrared OH nightglow emissions over Panhala. *J. Atmos. Sol.–Terr. Phys*., 2003, **65**, 1329–1335.
9. Midya, S. K. and Ghosh, S. N., Seasonal variations of OI 6300 Å night airglow emission at Calcutta and other stations and its covariation with OI 5577 Å emission. *Earth, Moon Planets*, 1994, **66**(2), 145–152; DOI: 10.1007/BF00644128.
10. Terra, P. M., Sobral, J. H. A., Abdu, M. A., Souza, J. R. and Takahashi, H., Plasma bubble zonal velocity variations with solar activity in the Brazilian region. *Ann. Geophys*., 2004, **22**, 3123–3128.
11. Mukherjee, G. K., Carlo, L., Mahajan, S. H. and Patil, P. T., First results of all-sky imaging from India. *Earth Planets Space*, 1998, **50**, 119–127.
12. Sahai, Y. P., Fagundesb, R. and Bittencourta, J. A., Transequatorial F-region ionospheric plasma bubbles: solar cycle effects. *J. Atmos. Sol.–Terr. Phys.*, 2000, **62**, 1377–1383.
13. Pimenta, A. A. *et al.*, Ionospheric plasma bubble zonal drift: A methodology using OI 630 nm All-Sky imaging system. *Adv. Space Res.*, 2001, **27**(6–7), 1219–1224.
14. Chung, J.-K., Kim, Y. H., Won, Y.-I. and Lee, B. Y., Observation of atmospheric waves in the OH airglow layer with an All-Sky camera. *J. Kor. Meteorol. Soc.*, 2003, **39**(3), 359–368.
15. Mukherjee, G. K., Airglow and other F-layer variations in the Indian sector during the geomagnetic storm of 5–7 February 2000. *Earth Planets Space*, 2006, **58**, 623–632.
16. Seker, I., Mathews, J. D., Wiig, J., Gutierrez, P. F., Friedman, J. S. and Tepley, C. A., First results from the Penn State All-Sky Imager at Arecibo Observatory. *Earth Planets Space*, 2007, **59**, 165–176.
17. Martinis, C., Eccles, J. V., Baumgardner, J., Manzano, J. and Mendillo, M., Latitude dependence of zonal plasma drifts obtained from dual-site airglow observations. *J. Geophys. Res. A*, 2003, **108**(3), 1129; doi: 10.1029/2002JA009462.
18. Martinis, C., Baumgardner, J., Wroten, J. and Mendillo, M., Seasonal dependence of MSTIDs obtained from 630.0 nm airglow imaging at Arecibo. *Geophys. Res. Lett*., 2010, **37**, L11103; doi: 10.1029/2010GL043569.
19. Rajesh, P. K., Liu, J. Y., Sinha, H. S. S. and Banerjee, S. B., Appearance and extension of airglow depletions. *J. Geophys. Res.*, 2010, **115**, A08318; doi: 10.1029/2009JA014952.
20. Garcia, F. J., Taylor, M. J. and Kelley, M. C., Two-dimensional spectral analysis of mesospheric airglow image data. *Appl. Opt.*, 1997, **36**, 29.
21. Kubota, M., Fukunishi, H. and Okano, S., Characteristics of medium- and large-scale TIDs over Japan derived from OI 630-nm nightglow observation. *Earth Planets Space*, 2001, **53**, 741–751.
22. Pragati Sikha, R., Parihar, N., Ghodpage, R. and Mukherjee, G. K., Observations of gravity waves in the upper mesosphere region by near infrared airglow imaging. *Curr. Sci*., 2010, **98**(3), 392–397.
23. Weber, E. J., Buchau, J. and Moore, J. G., Airborne studies of equatorial F layer ionospheric irregularities. *J. Geophys. Res. A*, 1980, **85**(9), 4631–4641.
24. de Paula, E. R. *et al.*, Ionospheric irregularity zonal velocities over Cachoeira Paulista. *J. Atmos. Sol.–Terr. Phys*., 2002, **64**, 1511–1516.
25. Fejer, B. G., Scherliess, L. and de Paula, E. R., Effects of the vertical plasma drift velocity on the generation and evolution of equatorial spread F. *J. Geophys. Res*., 1999, **104**, 19859–19870.
26. Daniela, C. S. A., Sobral, J. H. A., Abdu, M. A., Castilho, V. M., Takahashi, H., Medeiros, A. F. and Buriti, R. A., Theoretical and experimental zonal drift velocities of the ionospheric plasma bubbles over the Brazilian region. *Adv. Space Res*., 2006, **38**, 2610–2614.
27. Haerendel, G. and Eccles, J. V., The role of the equatorial electrojet in the evening ionosphere. *J. Geophys. Res*., 1992, **97**, 1181–1192.
28. Eccles, J. V., A simple model of low-latitude electric fields. *J. Geophys. Res*., 1998, **103**, 26699–26708.
29. Abdu, M. A., Batista, I. S., Takahashi, H., MacDougall, J., Sobral, J. H. A., Medeiros, A. F. and Trivedi, N. B., Magnetic disturbance induced equatorial plasma bubble development and dynamics: a case study in Brazilian sector. *J. Geophys. Res. A*, 2003, **108**(2), 1449; doi: 10.1029/2002JA009721.
30. Sobral, J. H. A. *et al.*, Westward drift velocities of the ionospheric plasma bubbles over the Brazilian region. In 11th International Symposium on Equatorial Aeronomy, Taipei, Taiwan, 9–14 May 2005.

ACKNOWLEDGEMENTS. D.P.N. thanks DST-PURSE for research assistantship. The nightglow observations at Kolhapur were carried out under scientific MoUs between Shivaji University, Kolhapur and Indian Institute of Geomagnetism, Navi Mumbai. We thank Mr R. B. Mane (J. B. Patil High School, Kolhapur) and Mr A. Valkunde for useful discussions on airglow geometry.

Received 13 January 2013; revised accepted 25 March 2013